

Olav Hagestad Nag

Intrabinary Shocks in Spider Pulsars

Bachelor's thesis in Physics
Supervisor: Karri Iiro Iisakki Koljonen
April 2024

Norwegian University of Science and Technology
Faculty of Natural Sciences
Department of Physics



Abstract

Neutron stars in binary systems are hotbeds of high-energy phenomena. As the orbital separation to their companion star lessens over a long timescale, the neutron star can start "sucking in" (accreting) matter from its companion star. In spider pulsars, this accretion process has gone on for long enough for the companion to have a very low mass and the neutron star to have gained enough angular momentum to rotate with a period of < 30 ms. This rotation, along with its magnetic field, powers a strong particle wind that ablates the companion. At the pressure balance point between this pulsar wind and the companion's stellar wind, a so-called intrabinary shock forms, luminous in X-rays and γ -rays. In this bachelor thesis, I outline the physical theory behind intrabinary shocks. I then summarize the evidence for their existence, considering observations in the X-ray and γ -ray band. Lastly, I discuss areas of ongoing investigation within the field of intrabinary shocks, such as γ -ray emission at TeV energies, magnetic pressure as an alternative to gas pressure in the formation of the intrabinary shock, the effect of pulsar irradiation on the stellar wind, and different models for intrabinary shock particle acceleration.

Contents

1	Introduction	1
1.1	Neutron stars	1
1.2	Pulsars and MSPs	1
1.3	Black widows and other spider pulsars	3
2	Basics of the intrabinary shock model	7
2.1	Pulsar wind	7
2.2	Stellar wind	8
2.3	The intrabinary shock	9
3	Observational evidence	13
3.1	X-ray spectral shape	13
3.2	X-ray lightcurve modulation	13
3.3	Gamma-ray evidence	16
4	Further research	19
4.1	High energy and very high energy gamma-ray emission	19
4.2	Shock acceleration vs. magnetic reconnection	20
4.3	Intrinsic vs. induced companion wind	20
4.4	Gas pressure vs. magnetic pressure	21
5	Summary	23
	Bibliography	25

Chapter 1

Introduction

1.1 Neutron stars

Neutron stars (NS) are compact objects usually formed when a large main-sequence (what one might call "normal") star runs out of fusion material in its core, collapsing under gravity without radiation pressure from fusion to stop it, creating a shockwave that flings the majority of the star's mass outwards in a bright event known as a supernova. Meanwhile, the remaining core collapses to a sufficient density for protons and electrons to fuse into neutrons, hence the name neutron star. NS are thought to have an initial mass of around $1.1 - 1.7 M_{\odot}$ and initially retain the angular momentum L of the progenitor core. However, since their radius is only $R_{NS} \simeq 10^6 \text{ cm} \simeq 10^{-5} R_{\odot}$ and $L \propto R$, they have a far shorter rotation period P than the progenitor. The extreme conditions of NS are difficult, if not impossible to recreate in a lab, and as such many aspects of them remain mysterious. For example, the equation of state describing the interior of an NS is not yet known.

1.2 Pulsars and MSPs

Pulsars, first discovered by Hewish et al. (1968), are NS that pulse in the radio spectrum with extreme regularity, as the hotspots at their magnetic poles are pointed towards Earth once per rotation period. As more pulsars were found, some were discovered to have $< 30 \text{ ms}$ rotation periods, in some cases 1.5 ms or less, and this population now makes up a significant percentage of total known pulsars. The rotation speed of all these *millisecond pulsars* (MSPs) seems highly implausible to come only from the angular momentum of the progenitor star, seeing as known young pulsars have longer periods, like the Crab pulsar ($\tau_{age} \simeq$

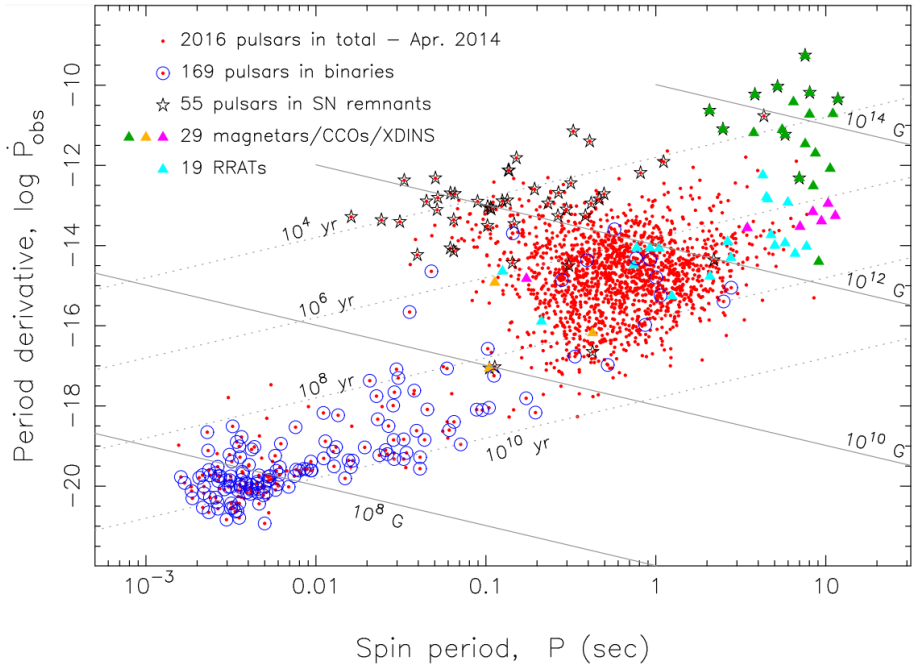


Figure 1.1: Pulsar spin period P versus spin period time derivative \dot{P} plotted for all 2016 pulsars in the ATNF pulsar catalogue as of April 2014. The catalogue lists 3534 pulsars as of April 2024, but the general picture is the same. The diagonal lines indicate characteristic age τ_c and magnetic field strength B . The MSP population is seen in the bottom left, relatively isolated from the main population, and is clearly where most binary pulsars are found. From Tauris (2015).

10^3 yr) with $P = 33$ ms, and the Vela pulsar ($\tau_{age} \simeq 10^4$ yr) with $P = 89$ ms, and pulsars that young are not expected to constitute a large percentage of the total pulsar population in our galaxy with an age of $\sim 10^{10}$ yr. Instead, these pulsars are thought to have been "recycled", having gained angular momentum from the accretion of a companion star, a second star gravitationally bound to the pulsar in a binary star system. This is evidenced by the majority of MSPs being in binary systems (see Fig. 1.1).

One initial hole in the model of recycling by accretion was the observation of MSPs without a companion. One might assume the accretion process could eventually let the pulsar "eat" up the entire companion, but accretion can only occur when the orbital separation of the binary is small enough for the companion

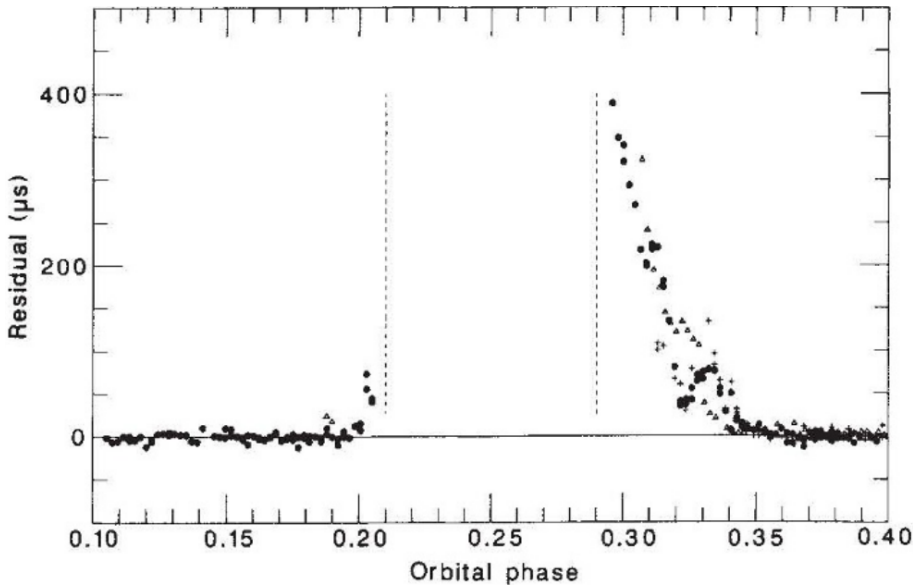


Figure 1.2: Plot of the radio delay in PSR B1957+20 over 0.3 full orbits. Between orbital phase 0.21 and 0.29, the radio signal is fully extinguished. From Fruchter et al. (1988).

Roche lobe to be filled (the region of space where the companion’s gravity is stronger than both the gravity of the NS and the centrifugal force of the binary orbit). The orbital separation shrinks over a long timescale as potential energy is lost to gravitational radiation, but the energy radiation rate $\langle \dot{E} \rangle$ is dependent on the NS and companion masses squared $M_{NS}^2 M_C^2$, so as the companion loses mass to accretion, the orbital separation will take longer to shrink, and thus the timescale over which the Roche lobe is filled increases. Seeing as accretion alone could not completely disintegrate the companion on the right timescales, there was a “missing link” in the evolution from actively accreting NS to lone MSPs.

1.3 Black widows and other spider pulsars

The missing link in the MSP evolution was found with the discovery by Fruchter et al. (1988) of the first *black widow pulsar*, PSR B1957+20 (with PSR being short for pulsar, and right ascension 19 h 57 min and declination 20° being the approximate stellar coordinates in the Besselian Epoch).

In B1957+20 and other black widows, a very light companion ($\sim 0.01 M_\odot$) in

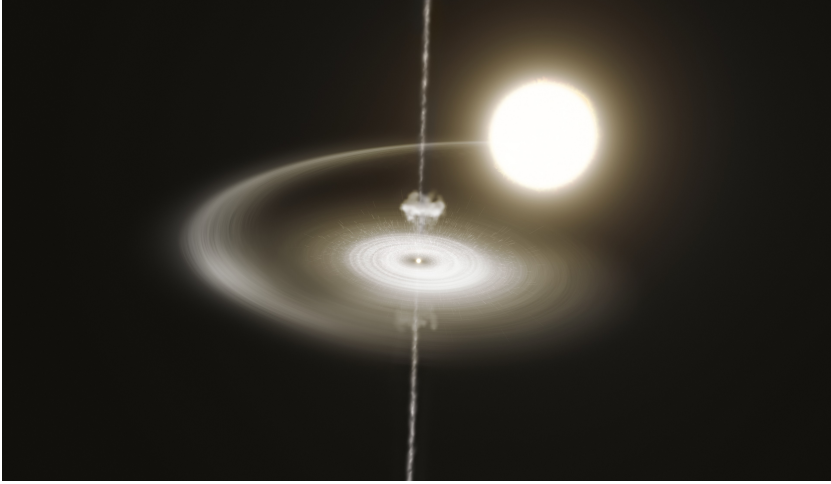


Figure 1.3: Artist’s illustration of the transitional redback PSR J1023+0038 in accretion phase, showing the companion, accretion flow, accretion disk, pulsar and magnetic pole jets. Image credit: ESO/M. Kornmesser.

a very close orbit (~ 1 day) is being ablated by a *pulsar wind*, a steady flow of electrons and positrons accelerated from the pulsar by a strong electric potential created by its rotation and magnetic field. This evaporation process is observed through a noticeable delay in the pulsar’s radio signal in comparison to the best-fit model, occurring a few minutes preceding and following the companion’s eclipse of the pulsar, with the delay after the eclipse being especially noticeable (see Fig.1.2). This is because electromagnetic radiation has a slower average speed through a medium (like gas) than through vacuum, due to the photons being scattered, creating longer paths for the individual photons to get through the cloud. When we observe this effect to be stronger after the companion star has passed in front of the pulsar, it indicates that there is a large cloud of ablated gas trailing behind the companion due to Coriolis effect. This ablation and presumed inevitable destruction, in addition to the mass disparity, inspired the name black widow, coined by Eichler & Levinson (1988), after a type of spider where the female eats its far smaller partner when mating.

This ablation also occurs in the related pulsar class called redbacks (named by Roberts (2011) after a species in the same genus as black widow spiders), distinguished from black widows primarily by a larger canonical companion mass of $0.1 M_{\odot}$, in addition to a somewhat larger variance in orbital period (still mostly < 1 day, but occasionally above). Redbacks are usually considered to be

the progenitors of black widows, with the higher companion mass indicating that they are earlier in the ablation process. This is further evidenced by redbacks having been observed switching between an accretion state and an ablation state where the radiation pressure of the pulsar is too strong for accretion, for example in PSR J1023+0038 (J for Julian epoch), shown in Fig. 1.3, which is often considered the canonical redback, like B1957+20 is for black widows. Black widows, redbacks and two smaller classes, tidarren pulsars (a sub-group of black widows characterised by very small companion mass and short orbital period, coined by Romani et al. 2016) and huntsman pulsars (characterised by giant companions, coined by Swihart et al. 2018) are collectively known as spider pulsars (spiders). These are found both in our galaxy and in globular clusters, clusters of stars orbiting our galaxy, though the evolutionary process in globular clusters may differ from the process described here.

Since 2008, the population of confirmed galactic spiders has gone from 4 (Fruchter et al. 1988; Stappers et al. 1996; Burgay et al. 2006; Archibald et al. 2009) to 56 (Koljonen & Linares 2023), largely thanks to the 2008 launch of the Fermi Gamma-ray Space Telescope. The Fermi-LAT (Large Area Telescope), the main instrument on the Fermi satellite, has discovered many unidentified sources of γ -rays, which radio telescopes could then check for the periodic radio signals of a pulsar. This explosion of possible targets of study presents enormous opportunities for deeper study of spiders. It can aid in answering questions like the NS equation of state, due to spider pulsars being among the most massive known neutron stars (thanks to accretion), ruling out candidate equations of state that predict a low maximum NS mass. The population explosion also provides ample targets for study of the phenomenon known as intrabinary shocks.

Intrabinary shocks (IBS) are non-thermal X-ray and γ -ray emitters found in spiders, where ultrarelativistic particles emitted from the pulsar interact with the companion stellar wind, accelerating particles within a magnetic field, producing high-energy radiation. The location of the shock between the pulsar and the companion, in addition to the relativistic velocity of the shocked particles following the shock tangent results in the observed emission varying periodically with the orbit, helping to distinguish the IBS radiation from other high-energy emitters in spider pulsars. The existence of IBS was postulated soon after the discovery of B1957+20 (Phinney et al. 1988; Harding & Gaisser 1990; Arons & Tavani 1993), and later confirmed by observations (see Chapter 3).

In this thesis I will discuss the model of intrabinary shocks in spider pulsars and the observations that infer their existence, focusing solely on spiders in the Galactic field. In Chapter 2, I will review the basics of the physical model behind intrabinary shocks. I will then consider the evidence for IBS in the X-ray band and the γ -ray band (Chapter 3). Finally, I will consider some open questions for further research (Chapter 4), and summarise in Chapter 5.

Chapter 2

Basics of the intrabinary shock model

As mentioned above, IBS occur at the pressure balance point between the pulsar wind and the stellar wind of the companion star in a spider pulsar. In this chapter, I will give a brief overview of stellar and pulsar winds, and the physical model of the IBS (under the assumption that the companion pressure stems from its wind).

2.1 Pulsar wind

To first approximation, a pulsar can be considered as a rotating magnetic dipole. The rotation induces an electric field of strength

$$E = \frac{\omega R_{NS} B_{NS}}{c}, \quad (2.1)$$

where $\omega = \frac{2\pi}{P}$ is the angular velocity, c is the speed of light in vacuum and B_{NS} is the magnetic field strength. The electric potential difference created is then

$$\Delta V = R_{NS} E = \frac{\omega R_{NS}^2 B_{NS}}{c} \quad (2.2)$$

(Cerutti 2018). Assuming a typical binary MSP (see Fig. 1.1) with $B_{NS} = 10^8$ G, $P = 5$ ms, and $R_{NS} = 10^6$ cm, the maximum kinetic energy of an electron or proton leaving the pulsar surface will be $K = e\Delta V \simeq 40$ GeV. This corresponds to a velocity much larger than the pulsar surface escape velocity $v > v_e = \sqrt{\frac{GM_{NS}}{R_{NS}}} \simeq 0.5c$, even for a proton. The pulsar should then emit a

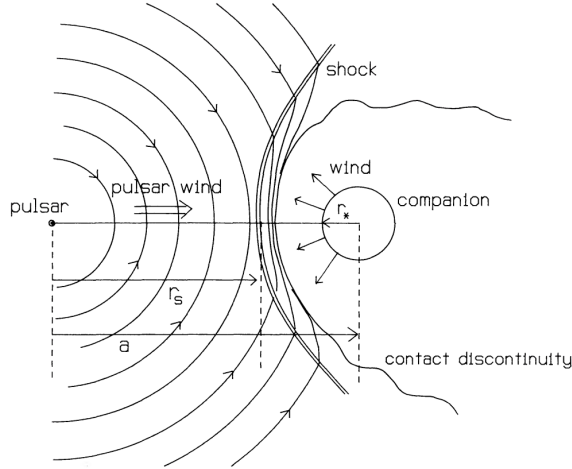


Figure 2.1: Overview of the IBS and its factors in PSR B1957+20. Pulsar wind meets the companion wind in a shock at a distance r_s from the pulsar. In most black widows, it can be assumed that $r_s \simeq a - r_* \simeq a$, where a is the orbital separation and r_* is the radius of the companion star. From Harding & Gaisser (1990).

steady stream of low-mass, high-energy particles. As these particles leave the pulsar, some of their kinetic energy is lost by spontaneously producing electron-positron pairs, and these pairs are thought to constitute the majority of the emitted pulsar wind.

2.2 Stellar wind

Stellar wind can be assumed to occur in the companion stars of all spider pulsars. In any well-mixed atmosphere (although heat exchange and convection flows can complicate the picture), the highest temperature material will generally tend to rise to the top. In the case of a star, some ions and electrons in the atmospheric plasma gain enough kinetic energy to escape the star's gravitational field. Collisions with other particles in the plasma contribute to this energy gain, but the full process is not completely understood even in our own Sun and is thought to involve a magnetic component. In spider companions, there is also the additional factor of strong irradiation from the pulsar, heating the stellar atmosphere, which could drive a much stronger stellar wind than would otherwise be possible, see section 4.3.

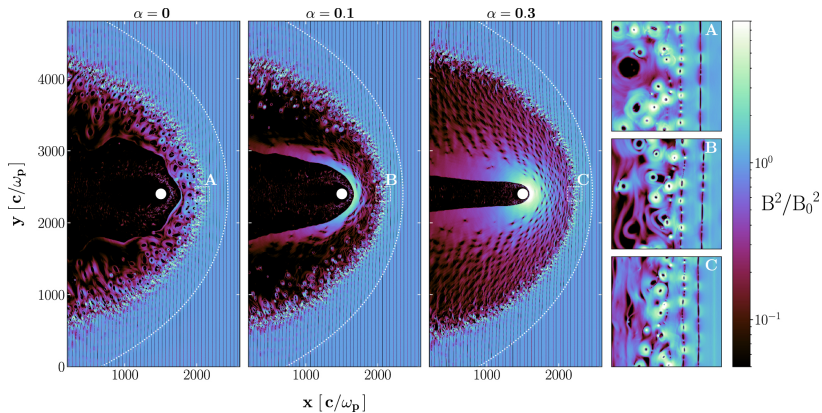


Figure 2.2: Numerical model of the IBS around a companion (assuming a magnetic reconnection scenario) for three values of the spectral index α , which measures the pulsar’s radiative flux density per unit frequency. The central white dot is the pulsar companion, and the coloring denotes the magnetic energy density, alternating in a striped pattern in the incoming wind, and then becoming more turbulent near the companion. Shown on the right is a zoomed-in view of the reconnection zones. From Cortés & Sironi (2022)

2.3 The intrabinary shock

The winds emanating from the pulsar and its companion can be regarded as two flows in a very diffuse magnetic fluid (magnetohydrodynamics). In the intrabinary space, these flows are antiparallel, and where they exert an equal amount of pressure, a shock forms (see Fig. 2.1). In this shock, the combination of relativistic charged particles and a strong magnetic field causes the particles to gyrate around magnetic field lines, radiating (synchrotron radiation) as they alter their momentum vector. In the case of an IBS, this synchrotron radiation is emitted at X-ray and γ -ray wavelengths. The exact mechanism by which particles are accelerated to sufficient velocity in the IBS is still under debate. The main two mechanisms that produce X-ray and γ -ray synchrotron radiation are diffusive shock acceleration and magnetic reconnection.

In diffusive shock acceleration, particles scatter randomly after crossing the IBS, some particles scattering back towards the shock resulting in a second crossing. Subsequent crossings can occur, and the particle will gain kinetic energy each time it passes through the IBS, resulting in strong particle acceleration. In magnetic reconnection, the pulsar wind is assumed to have a “striped” structure where from the perspective of an observer close to the pulsar, the charge

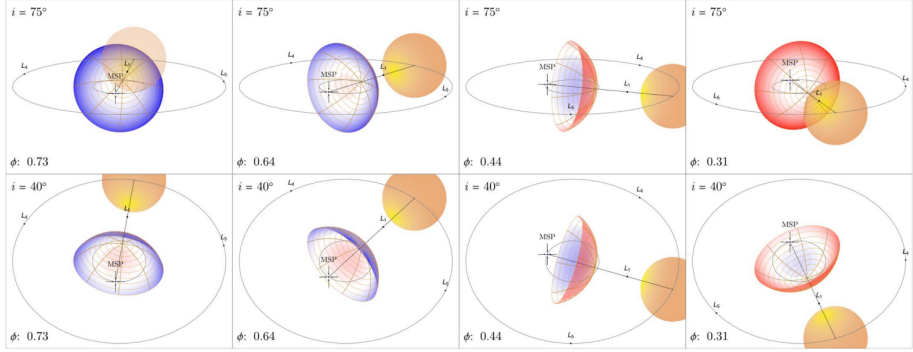


Figure 2.3: model of an IBS wrapping around the pulsar seen from inclination angles $i = 75^\circ$ and $i = 40^\circ$ at orbital phases $\phi = 0.73$, $\phi = 0.64$, $\phi = 0.44$ and $\phi = 0.31$. Orbital phase is defined such that the pulsar is in front of the companion at $\phi = 0.75$, and the opposite case is at $\phi = 0.25$. From van der Merwe et al. (2020).

of the emitted wind will alternate periodically. These alternating charges collide (”reconnecting”) as the wind is slowed down by the shock, creating magnetically turbulent zones (see Fig. 2.2) where individual particles can be accelerated to relativistic speeds. Both processes produce X-ray emission following a power-law curve (i.e. a function on the form $F_\nu \propto \nu^\Gamma$, where ν is the photon frequency, and Γ is called the photon index), but magnetic reconnection has a harder spectrum (lower Γ), and thus observational discrimination is possible.

Regardless of the acceleration process, the velocity of the shocked particles is expected to follow the shock tangent to some extent. Consequently, for an observer looking straight at the shock, the shocked particles will be moving towards the observer at an appreciable fraction of c , giving their emission a length-contracted wavelength. This means their emission will have higher energy, a phenomenon called Doppler beaming. The effect is shown with blue (for particles moving towards the observer) and red (for particles moving away) colouring in Fig. 2.3.

The relative strength of the two winds affects both the shape and location of the shock. The location of the shock as a ratio of pulsar distance r_s to orbital separation a is given by

$$\frac{r_s}{a} \simeq \frac{1}{1 + \sqrt{\eta}}, \quad (2.3)$$

clearly depending only upon the factor $\eta = \frac{\dot{M}_w v_w c}{\dot{E}}$, where \dot{M}_w is the rate of companion mass lost as wind, v_w is the speed of the companion wind, and \dot{E} is the

rate of pulsar energy lost as wind (Dubus 2015). Of course, this assumes isotropic stellar and pulsar wind, which is no trivial assumption, given the hemispherical disparity of the companion wind from pulsar irradiation, and the inherent anisotropy of the rotating dipole that is typically used to model the pulsar.

The shape of the IBS can be divided into two categories, corresponding to the two main spider classes (though perhaps not perfectly, see section 4.4). In black widows, the pulsar wind dominates ($\eta \ll 1$), and the shock wraps around the companion in a roughly parabolic shape (see Fig. 2.2). In redbacks, the companion has a stronger wind due to being larger in size, and observations (Gentile et al. 2014; Hui et al. 2014; Al Noori et al. 2018; Kong et al. 2018) suggest that it is strong enough for a pulsar-wrapping shock.

Chapter 3

Observational evidence

The orbitally modulated X-ray emission and hard spectra detected from spiders remain the most significant piece of evidence for IBS. There are two primary characteristics of the X-ray emission that yield information about the system, the spectral shape and the lightcurve (flux over time). Orbitally modulated γ -ray emission is also an indicator of the IBS, but this has not been detected with as high significance and hence is not as strong evidence.

3.1 X-ray spectral shape

To infer the spectral shape of the radiation, observational data is fitted with one or more spectral models, which in turn imply what emission processes are at work. A blackbody model is one example, and some spiders exhibit observable amounts of X-ray blackbody radiation, but a power-law model component is usually also needed (see Fig. 3.1). There are several potential sources of X-ray emission in spiders. Thermal (blackbody) radiation is usually assumed to come from the pulsar magnetic poles, while non-thermal radiation is assumed to come from either the pulsar magnetosphere or the IBS, both emitting with a power-law spectrum, but with differing photon indices Γ . Despite this, the primary way to distinguish the two is by looking at the phase-folded X-ray lightcurve, the amount of X-ray luminosity over the course of the binary orbit.

3.2 X-ray lightcurve modulation

In any binary system, the emission is generally expected to vary over the course of one orbit, though this depends on the inclination angle of the system. If the

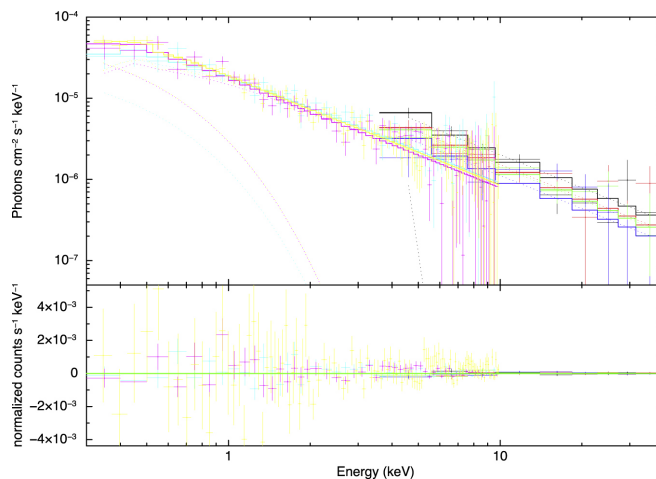


Figure 3.1: Top: the X-ray spectrum of redback PSR J2129-0429 obtained with NuSTAR (3-40 keV) and XMMNewton (0.3-10 keV) X-ray satellites, showing the X-ray photon flux for different photon energies. The spectrum has been fitted with an absorbed power law and neutron star atmosphere, and the colours represent different observations and instruments. Bottom: residuals from the fitting, showing the difference between the model and the data at each energy bin. From Al Noori et al. (2018).

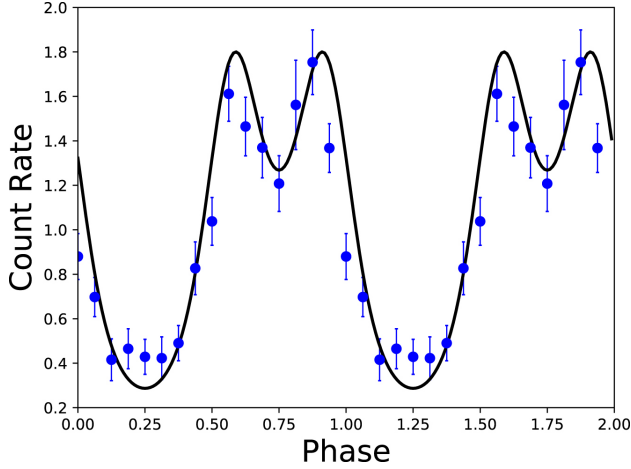


Figure 3.2: Phase-folded, Normalised count rate variation of X-rays of energies 3-40 keV plotted over two full orbits of the redback PSR J2129-0429. The double peaks are closer to superior conjunction of the companion ($\phi = 0.75$) than inferior conjunction of the companion, indicating that the shock wraps around the pulsar. From Kong et al. (2018).

inclination is $i = 0^\circ$, then the orbit (as viewed from Earth) is seen directly "from above". If the inclination is $i = 90^\circ$, then the system is seen "edge on". In high inclination cases in spiders with companion-wrapping shocks, dimming of both the magnetosphere and the IBS is expected at inferior conjunction of the companion (when the companion is directly in front of the pulsar). However, a peak right before and after inferior conjunction of the companion (due to Doppler beaming) is expected only from IBS, and this is exactly what is observed in many spiders (see Fig. 3.2).

Of course, not all systems are seen close to edge-on. In spiders observed at a somewhat lower inclination (exactly how low depends on the precise shape of the shock, which might vary from system to system), the line of sight will run tangent to the shock, producing a broad "hump" (see Fig. 3.3) instead of two isolated peaks. These expectations remain the same for the scenario where the IBS wraps around the pulsar, though instead the double peaks or hump occur around superior conjunction of the companion (when the companion is directly behind the pulsar).

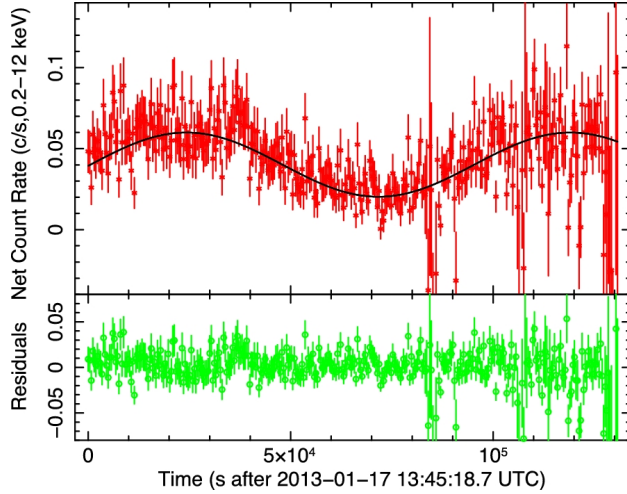


Figure 3.3: X-ray count rate (of energies 0.2-12 keV) over time in the redback PSR J1306-40, showing a ”hump” structure (though somewhat obscured by flares in the latter half of the observation period). The orbital period is $\sim 9.5 \times 10^4$ s, and $t = 0$ is at inferior conjunction of the companion. From Linares (2018).

3.3 Gamma-ray evidence

Given that the explosion in the known spider population largely came due to γ -ray observations from Fermi-LAT, it should not be surprising that γ -ray emission is ubiquitous among spider pulsars. However, to begin with, all observed γ -ray emission was assumed to come from the pulsar magnetosphere, not the IBS, as the observed emission was not orbitally modulated. Wu et al. (2012) found some indication of orbital modulation, but this was below 3σ significance.

The first to observe orbital modulation above 3σ significance was Xing & Wang (2015), who found the γ -ray flux of black widow PSR J1311-3430 to vary roughly sinusoidally with the binary orbit period of the system. They observed a flux maximum at the superior conjunction of the companion, and a minimum at the inferior conjunction of the companion, suggesting an origin close to the companion (where one expects to find an IBS in a black widow), though with no apparent sign of Doppler beaming (double peaks). An et al. (2017) also found similar results for the same system. Ng et al. (2018) and An et al. (2018) (see Fig. 3.4) found the opposite modulation for redbacks PSR J2039-5618 and PSR J2241-5236 respectively, with the lightcurve peaking at the inferior conjunction of the companion. While An et al. (2018) interpret this as synchrotron emission from

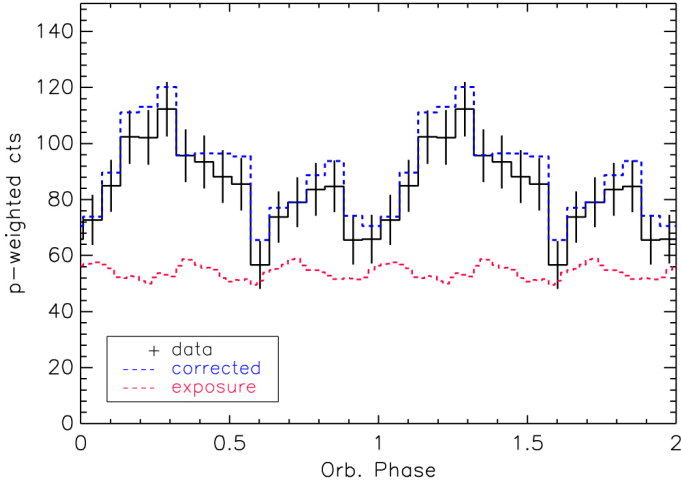


Figure 3.4: Phase-folded γ -ray lightcurve of energies 0.06-1 GeV of black widow PSR J2241-5236 plotted for two full orbits. Inferior conjunction of the companion is at $\phi = 0.25$, around where the curve peaks. When compared to 3.2, the pattern here is clearly less pronounced, the magnitude of the variation being much closer to the magnitude of the error bars. From An et al. (2018).

an IBS seen at moderate inclination, Ng et al. (2018) interpret it as companion thermal photons that meet the high kinetic energy particles of the pulsar wind and get momentum transferred to them via the inverse Compton effect.

It is important to note that all these discoveries have a significance below 5σ for there even being any orbital modulation, much less modulation following some specific curve.

Chapter 4

Further research

Despite the large amount of confirmed spider systems and evidence of IBS emission from them, there are still many unanswered questions regarding IBS. In this chapter, I will give a brief overview of some notable points of uncertainty: The γ -ray component of IBS emission, the acceleration mechanism of the IBS, the effect of pulsar irradiation on the companion wind, and finally the mechanism by which the companion exerts pressure against the pulsar wind.

4.1 High energy and very high energy gamma-ray emission

As discussed in section 3.3, the γ -ray emission observed from spider pulsars does not yet have conclusive evidence of an orbitally modulated component, despite IBS models predicting their existence (van der Merwe et al. 2020). The same paper also predicts TeV energy γ -ray emission from inverse Compton scattering of companion blackbody radiation, the same mechanism that Ng et al. (2018) used to explain their observation of orbitally modulated 0.1-3 GeV γ -rays. TeV γ -ray IBS emission has yet to be searched for with any telescope, although this might change with the upcoming advent of the Cherenkov Telescope Array, which will be more sensitive than any current telescopes to TeV γ -rays.

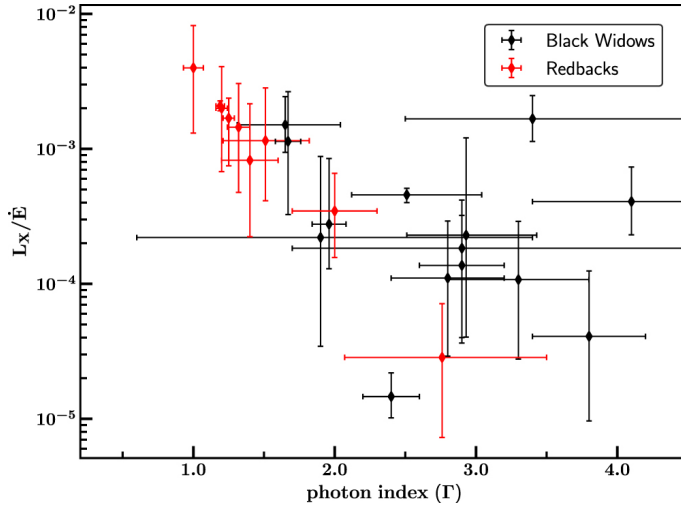


Figure 4.1: X-ray luminosity as a fraction of the total spin-down power plotted against photon index Γ for 14 black widows and 9 redbacks. Systems with a Γ significantly larger than 2 can be assumed to be dominated by thermal emission. From Swihart et al. (2022).

4.2 Shock acceleration vs. magnetic reconnection

Already from the first proposal of IBS in Phinney et al. (1988), it was recognised that two separate processes could produce orbitally modulated X-ray and γ -ray emission: Magnetic reconnection and diffusive shock acceleration. Kandel et al. (2019) give different expectations for the spectra of these two processes, with $\Gamma \geq 1.5$ for diffusive shock acceleration, while for magnetic reconnection Γ may be as low as 1.

The possibility exists that the dominant mechanism may depend on the type of spider. As seen in Fig. 4.1, redbacks tend to have a harder spectrum, as is expected for magnetic reconnection, while black widows are more varied, but tend to have softer spectra.

4.3 Intrinsic vs. induced companion wind

The companion stellar wind, which has in this work been assumed as the force acting against the pulsar wind pressure in an IBS, may be substantially or even

dominantly driven by the irradiation from the pulsar. This radiation from the pulsar can impart a significant amount of energy to the companion surface, and since the companion can be assumed to be tidally locked (i.e. the same side always faces the pulsar), this can lead to a large hemispherical temperature asymmetry. For example, in the companion of the redback PSR J2339-0533, the day-side temperature is ~ 6900 K, while the night-side temperature is ~ 2900 K (Romani & Shaw 2011). This may drive stronger stellar wind, which according to Wadiasingh et al. (2018) is necessary for the stellar wind to be strong enough to push back against the pulsar wind. However, the potential magnitude of the effect is yet to be determined.

4.4 Gas pressure vs. magnetic pressure

Finally, the assumption that stellar wind is the factor balancing the pulsar wind is not necessarily needed. The magnetosphere of the companion may be strong enough to exert the opposing pressure on its own, possibly even strong enough for a pulsar-wrapping shock. This has been suggested by Swihart et al. (2022) to be the case with PSR J1311-3430 and PSR J1653-0158, two black widows whose X-ray luminosity and hardness are close to that of most redbacks (see Fig. 4.1), with J1311-3430 having $\Gamma = 1.67 \pm 0.09$. and $L_X = 55.7^{+39.7}_{-74.3}$, and J1653-0158 having $\Gamma = 1.65^{+0.34}_{-0.39}$ and $L_X = 18.1^{+6.8}_{-11.2}$. While it is worth noting that these pulsars constitute two out of three members of the tidarren subclass of black widows, the third member, PSR J0636+5129, does not share their behaviour, being both significantly weaker ($L_X = 0.08^{+0.04}_{-0.03}$) and softer ($\Gamma = 2.4 \pm 0.2$).

Chapter 5

Summary

In this thesis, I have given an introduction to the field of intrabinary shocks in spider pulsars, outlining the processes of stellar and pulsar winds, and their interaction in the gas pressure scenario. I have considered the observational expectations from IBS in terms of X-ray spectra and orbital modulation, and given an overview of spider observations displaying orbitally modulated γ -ray emission. Lastly, I have looked at current areas of investigation in IBS, such as TeV γ -ray emission, the question of whether the IBS synchrotron radiation is produced by diffusive shock acceleration or magnetic reconnection, the impact of the pulsar irradiation of the companion on its stellar wind, and the possibility of companion magnetic pressure as the factor balancing the pulsar wind.

Bibliography

- Al Noori, H., Roberts, M. S. E., Torres, R. A., McLaughlin, M. A., Gentile, P. A., Hessels, J. W. T., Ray, P. S., Kerr, M., and Breton, R. P. (2018). X-ray and optical studies of the redback system psr j2129-0429. *The Astrophysical Journal*.
- An, H., Romani, R. W., Johnson, T., Kerr, M., and Clark, C. J. (2017). High-energy Variability of PSR J1311-3430. *The Astrophysical Journal*.
- An, H., Romani, R. W., and Kerr, M. (2018). Signatures of intra-binary shock emission in the black widow pulsar binary psr j2241-5236. *The Astrophysical Journal Letters*.
- Archibald, A. M., Stairs, I. H., Ransom, S. M., Kaspi, V. M., Kondratiev, V. I., Lorimer, D. R., McLaughlin, M. A., Boyles, J., Hessels, J. W. T., Lynch, R., van Leeuwen, J., Roberts, M. S. E., Jenet, F., Champion, D. J., Rosen, R., Barlow, B. N., Dunlap, B. H., and Remillard, R. A. (2009). A Radio Pulsar/X-ray Binary Link. *Science*.
- Arons, J. and Tavani, M. (1993). High-energy emission from the eclipsing millisecond pulsar psr 1957+20. *The Astrophysical Journal*.
- Burgay, M., Joshi, B. C., D'Amico, N., Possenti, A., Lyne, A. G., Manchester, R. N., McLaughlin, M. A., Kramer, M., Camilo, F., and Freire, P. C. C. (2006). The Parkes High-Latitude pulsar survey. *Monthly Notices of the Royal Astronomical Society*.
- Cerutti, B. (2018). Particle acceleration and radiation in pulsars: New insights from kinetic simulations. In *Nuclear and Particle Physics Proceedings*.
- Cortés, J. and Sironi, L. (2022). Global kinetic modeling of the intrabinary shock in spider pulsars. *The Astrophysical Journal*.
- Dubus, G. (2015). Gamma-ray emission from binaries in context. In *Comptes rendus - Physique*.

- Eichler, D. and Levinson, A. (1988). On black widow evolutionary scenarios for binary neutron stars. *The Astrophysical Journal*.
- Fruchter, A. S., Stinebring, D. R., and Taylor, J. H. (1988). A millisecond pulsar in an eclipsing binary. *Nature*.
- Gentile, P. A., Roberts, M. S. E., McLaughlin, M. A., Camilo, F., Hessels, J. W. T., Kerr, M., Ransom, S. M., Ray, P. S., and Stairs, I. H. (2014). X-ray observations of black widow pulsars. *The Astrophysical Journal*.
- Harding, A. K. and Gaisser, T. K. (1990). Acceleration by pulsar winds in binary systems. *The Astrophysical Journal*.
- Hewish, A., Bell, J. S., Pilkington, J. D. H., Scott, P. F., and Collins, R. A. (1968). Observation of a rapidly pulsating radio source. *Nature*.
- Hui, C. Y., Tam, P. H. T., Takata, J., Kong, A. K. H., Cheng, K. S., Wu, J. H. K., Lin, L. C. C., and Wu, E. M. H. (2014). Exploring the x-ray and γ -ray properties of the redback millisecond pulsar psr j1723-2837. *The Astrophysical Journal Letters*.
- Kandel, D., Romani, R. W., and An, H. (2019). The synchrotron emission pattern of intrabinary shocks. *The Astrophysical Journal*.
- Koljonen, K. I. I. and Linares, M. (2023). A gaia view of the optical and x-ray luminosities of compact binary millisecond pulsars. *Monthly Notices of the Royal Astronomical Society*.
- Kong, A. K. H., Takata, J., Hui, C. Y., Zhao, J., Li, K. L., and Tam, P. H. T. (2018). Broad-band high-energy emissions of the redback millisecond pulsar psr j2129-0429. *Monthly Notices of the Royal Astronomical Society*.
- Linares, M. (2018). The 26.3-h orbit and multiwavelength properties of the ‘redback’ millisecond pulsar psr j1306-40. *Monthly Notices of the Royal Astronomical Society*.
- Ng, C. W., Takata, J., Strader, J., Li, K. L., and Cheng, K. S. (2018). Evidence on the orbital modulated gamma-ray emissions from the redback candidate 3fgl j2039.6-5618. *The Astrophysical Journal*.
- Phinney, E. S., Evans, C. R., Blandford, R. D., and Kulkarni, S. (1988). Ablating dwarf model for eclipsing millisecond pulsar 1957 + 20. *Nature*.
- Roberts, M. S. E. (2011). New black widows and redbacks in the galactic field. In *RADIO PULSARS: AN ASTROPHYSICAL KEY TO UNLOCK THE SECRETS OF THE UNIVERSE*.

- Romani, R. W., Graham, M. L., Filippenko, A. V., and Zheng, W. (2016). Psr j1301+0833: A kinematic study of a black-widow pulsar. *The Astrophysical Journal*.
- Romani, R. W. and Shaw, M. S. (2011). The orbit and companion of probable γ -ray pulsar j2339-0533. *The Astrophysical Journal Letters*.
- Stappers, B. W., Bailes, M., Lyne, A. G., Manchester, R. N., D’Amico, N., Tauris, T. M., Lorimer, D. R., Johnston, S., and Sandhu, J. S. (1996). Probing the Eclipse Region of a Binary Millisecond Pulsar. *The Astrophysical Journal Letters*.
- Swihart, S. J., Strader, J., Chomiuk, L., Aydi, E., Sokolovsky, K. V., Ray, P. S., and Kerr, M. (2022). A new flaring black widow candidate and demographics of black widow millisecond pulsars in the galactic field. *The Astrophysical Journal*.
- Swihart, S. J., Strader, J., Shishkovsky, L., Chomiuk, L., Bahramian, A., Heinke, C. O., Miller-Jones, J. C. A., Edwards, P. G., and Cheung, C. C. (2018). A multiwavelength view of the neutron star binary 1fgl j1417.7-4402: A progenitor to canonical millisecond pulsars. *The Astrophysical Journal*.
- Tauris, T. M. (2015). Millisecond pulsars in close binaries. *Rhenish Friedrich Wilhelm University of Bonn*.
- van der Merwe, C. J. T., Wadiasingh, Z., Venter, C., Harding, A. K., and Baring, M. G. (2020). X-ray through very high energy intrabinary shock emission from black widows and redbacks. *The Astrophysical Journal*.
- Wadiasingh, Z., Venter, C., Harding, A. K., Böttcher, M., and Kilian, P. (2018). Pressure balance and intrabinary shock stability in rotation-powered-state redback and transitional millisecond pulsar binary systems. *The Astrophysical Journal*.
- Wu, J. H. K., Kong, A. K. H., Huang, R. H. H., Takata, J., Tam, P. H. T., Wu, E. M. H., and Cheng, K. S. (2012). Discovery of γ -ray pulsation and x-ray emission from the black widow pulsar psr j2051-0827. *The Astrophysical Journal*.
- Xing, Y. and Wang, Z. (2015). Discovery of gamma-ray orbital modulation in the black widow psr j1311-3430. *The Astrophysical Journal Letters*.